Scaling of the Hall effects beyond the quantum resistance threshold in oxidized CoFeB

A. Gerber and G. Kopnov

Raymond and Beverly Sackler Faculty of Exact Sciences, School of Physics and Astronomy, Tel Aviv University, Ramat Aviv 69978, Tel Aviv, Israel

(Received 16 January 2017; revised manuscript received 24 April 2017; published 14 June 2017)

The ordinary and the extraordinary Hall effects were studied in gradually oxidized amorphous CoFeB ferromagnets over six orders of resistivity from the metallic to the strongly insulating regime. Polarity of the extraordinary Hall effect reverses, and the amplitude of both the ordinary and the extraordinary Hall effects increases quadratically with resistivity when resistance exceeds the quantum resistance threshold $h/2e^2$. The absolute value of the extraordinary Hall effect scales linearly with the ordinary one in the entire range over eight orders of magnitude between the metallic and the insulating states. The behavior differs qualitatively and quantitatively from the theoretically predicted and experimentally known behavior in other materials.

DOI: 10.1103/PhysRevB.95.214206

I. INTRODUCTION

The Hall effect is the major source of information on a type and density of charge carriers. Regretfully, our knowledge of the phenomenon in strongly disordered conductors is quite poor as experimental data are scarce and sometimes controversial. The reason is essentially technical: for any practical arrangement of electric contacts, there is an unavoidable geometrical mismatch in positioning of transverse to current (Hall) probes. Since longitudinal electric field is usually much larger than the transverse one, a relatively small Hall signal is hidden on a background of the longitudinal resistance noise. Thus, practically no data are available on the insulating side of the metal-insulator transition for resistivity exceeding $0.1-1\,\Omega$ cm. This absence of data does not reflect an absence of interest, as a number of puzzling phenomena, such as an existence of the Hall insulator state [1–3], double reversal of Hall effect polarity [4,5], and the giant Hall effect [6] were pointed out but remained unresolved. Availability of the extraordinary Hall effect (EHE) data in ferromagnetic systems is somewhat better, since the effect is usually much larger than the ordinary Hall effect and is easier to measure. An impression has been created that recent theoretical models [7–10] provide a satisfactory interpretation of all the existing data, excluding probably the giant EHE in granular ferromagnets [11]. Here we report on the experimental study of the ordinary and the extraordinary Hall effects in gradually oxidized amorphous CoFeB ferromagnets, where the effects appear to be remarkably large and measurable over six orders of resistivity from the metallic into the deep insulating regime. We found a number of unexpected and intriguing properties that include a crossover between the apparently Hall insulator state and the state with quadratically diverging Hall coefficient; a linear correlation between the ordinary Hall coefficient and the extraordinary Hall resistivity expanding from the metallic to the insulating state; and collapse of the accepted EHE scaling in the high resistivity limit. The crossover resistance where the unusual behavior starts is very close to the quantum resistance value.

II. EXPERIMENT

Recently we reported [12] on the development of partially oxidized amorphous CoFeB ferromagnetic films with resistivity variable between $100\,\mu\Omega$ cm to beyond $10^2\,\Omega$ cm, depending on the degree of oxidation. Thin films with thickness between 5 and 50 nm were fabricated by reactive rf magnetron sputtering from $Co_{40}Fe_{40}B_{20}$ target (ACI Alloys Inc.) on rectangular 5×5 mm^2 pieces of intrinsic GaAs substrate. Base pressure prior to deposition was about 2×10^{-7} torr, whereas deposition took place at 5×10^{-3} torr Ar atmosphere mixed with a controlled flow of either air or pure oxygen. The typical deposition rate was 0.1–0.2 nm/s. Resistivity is very sensitive to the presence of air and increases sharply when air partial pressure goes above 10^{-3} torr, that is about 1:5 ratio with argon. Structural analyses were done using x-ray diffraction, high-resolution transmission electron microscopy and time-of-flight secondary ion mass spectrometry. All samples deposited with and without air were found to be amorphous [12]. The resistance, magnetoresistance, and Hall effect were measured using the Van der Pauw protocol. The Hall effect and magnetization data discussed here were obtained at room temperature. The GaAs substrate we used was not conducting when tested by itself, and the sufficiently oxidized films were not conducting as well. We therefore excluded the possibility of current leakage and parallel conductance along the films and the substrate [13]. Magnetic characterization of the samples was done using a superconducting quantum interference device magnetometer.

Due to the amorphous structure, we did not succeed in extracting information on the topology of the oxidized samples: whether the material is homogeneous or heterogeneous, forming amorphous metallic clusters embedded within an amorphous insulating oxide. As will be discussed in the following, microscopic interpretation of the data might depend on this missing information.

III. RESULTS AND DISCUSSION

Figure 1 presents the field dependence of Hall resistance R_{xy} of two typical samples with lower (a) and higher (b) degrees of oxidation. Both samples are 10 nm thick; their resistivities are $11.5 \times 10^{-3}\,\Omega$ cm (a) and $1.4\,\Omega$ cm (b). Hall resistance R_{xy} in magnetic films can be presented as a superposition of the ordinary and the extraordinary Hall effects: $R_{xy} = V_{xy}/I = \rho_{xy}/t = (\rho_{OHE}B_z + \mu_0 R_s M_z)/t$, where ρ_{xy} is Hall resistivity, I is the current, t is the thickness,

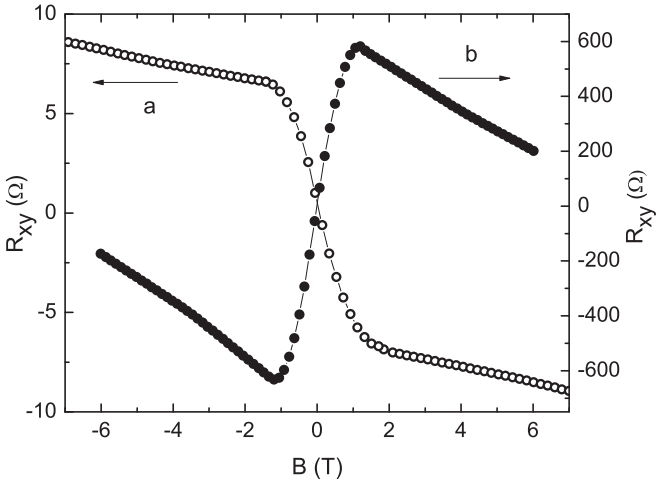

FIG. 1. Hall resistance R_{xy} of two 10-nm-thick samples with lower (a) and higher (b) degrees of oxidation as a function of applied magnetic fields. Resistivity is 11.5×10^{-3} Ω cm (a) and 1.4 Ω cm (b).

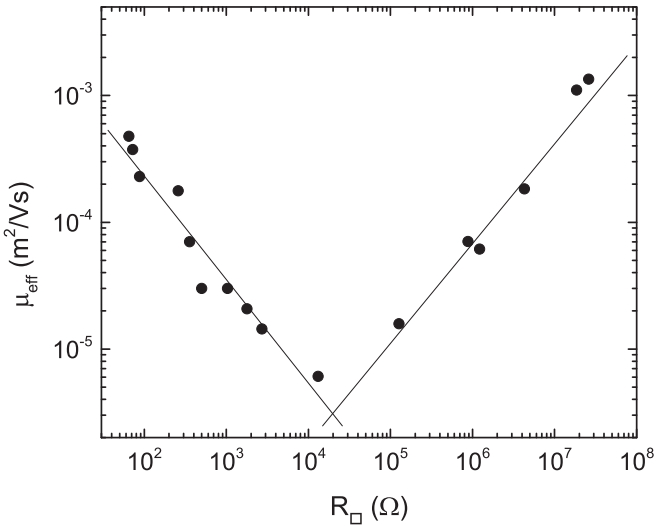

FIG. 3. The effective mobility of a series of 50-nm-thick samples as a function of sheet resistance. Straight lines are a guide to the eye.

ρ_{OHE} and R_s are the ordinary and the extraordinary Hall effect coefficients, and B_z and M_z are the normal-to-plane projections of magnetic field induction and magnetization, respectively. EHE resistivity ρ_{EHE} is defined as $\rho_{EHE} = \mu_0 R_s M_{z,\mathrm{sat}}$, where $M_{z,\mathrm{sat}}$ is the saturated out-of-plane magnetization. ρ_{EHE} is determined by extrapolation of the magnetically saturated high field linear portion of $R_{xy}(B)$ to zero field. The ordinary Hall effect coefficient ρ_{OHE} is determined by the high field slope in magnetically saturated state as $\rho_{OHE} = (dR_{xy}/dB)t$. ρ_{OHE} is constant in fields over at least 10 T range and is negative in all samples. The extraordinary Hall resistivity, dominant below 1 T, is negative in sample (a) and positive in the high resistivity samples (b).

Figure 2 shows the ordinary Hall effect coefficient ρ_{OHE} as a function of longitudinal resistivity ρ. Within the logarithmic

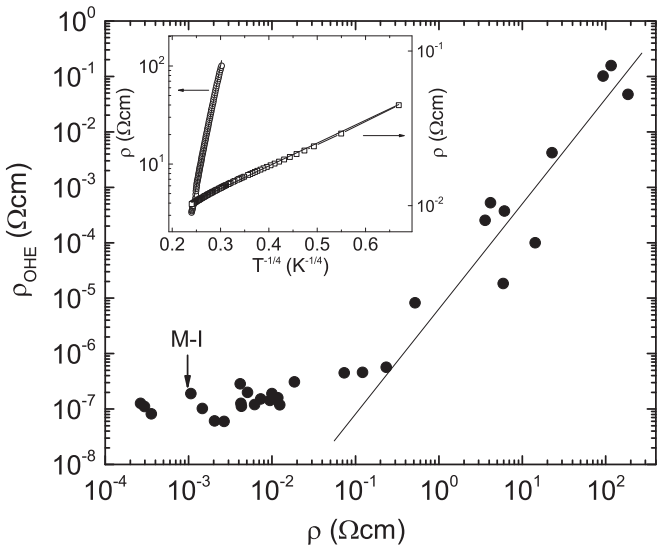

FIG. 2. The ordinary Hall effect coefficient as a function of longitudinal resistivity ρ. M-I indicates the metal-insulator transition. Inset: resistivity of two typical samples as a function of temperature, taken from Ref. [12]. Straight lines are a guide to the eye.

accuracy ρ_{OHE} increases slightly with an increase of resistivity below 10^{-1} Ω cm, and grows sharply as $\rho_{OHE} \propto \rho^2$ for $\rho > 10^{-1}$ Ω cm. ρ_{OHE} exceeds 10^{-1} Ω cm at $\rho = 10^2$ Ω cm, which is six orders of magnitude higher than in bulk amorphous CoFeB. Samples sputtered in a pure Ar atmosphere are metallic with a positive resistivity temperature coefficient at room temperature. Oxidized samples are insulator-like with resistivity increasing with decreasing temperature. A transition between the metallic-like and the insulator-like temperature dependencies occurs at a resistivity about 10^{-3} Ω cm, marked by the M-I arrow in the figure. A transition between the range with approximately constant Hall coefficient and the range in which $\rho_{OHE} \propto \rho^2$ takes place at about 10^{-1} Ω cm, well beyond the metal-insulator transition. The inset in Fig. 2 presents the resistivity temperature dependence of two samples: the first belonging to the constant Hall range and the second to the diverging one. Resistivity of both samples can be presented as $\rho = \rho_0 \exp(\frac{T_0}{T})^{1/4}$ with T_0 increasing from 150 K for sample 1 with room temperature resistivity 10^{-2} Ω cm to about 10^7 K for sample 2 with resistivity 3.2 Ω cm. Such temperature dependence of resistivity is consistent with the variable range hopping conductance model [14], but also with the temperature-assisted conductance in granular media [15].

To emphasize an unusual character of the high resistivity Hall coefficient we plot in Fig. 3 the effective Hall mobility μ_{eff} as a function of sheet resistance. μ_{eff} was calculated as $\mu_{\mathrm{eff}} = \sigma/qn^* = \rho_{OHE}/\rho$, where n^* is defined as an "effective" charge density. We use the terms "effective density" and "effective mobility," since the classical definition $\rho_{OHE} = \frac{1}{nq}$, where q is electric charge and n is a number of free electrons per unit volume, is not generally correct for hopping charge transport [16,17]. The effective mobility has a unique V shape as a function of resistance: decreasing linearly with resistance in the "low" resistance range and increasing linearly at high resistances. As a rule, mobility decreases with increasing disorder and respectively increasing resistivity. Thus, a linear increase of mobility in the high resistance limit is remarkable. Notably, resistance of the crossover between the decreasing

and increasing mobility ranges is close to the quantum resistance value $R_Q = h/2e^2 \approx 12.9$ kΩ.

Hall effect in the hopping conductance regime was calculated in a number of works [17–23]. It is commonly considered that in macroscopically homogeneous material the hopping Hall effect is related to self-interference of the electron wave function, propagating along different paths with at least three localization centers taken into account [17]. Mainly, it was the temperature variation of the effect that has been addressed. The power-law relation between the Hall coefficient and longitudinal resistance was predicted to be $\rho_{OHE} \propto \rho^{\gamma}$, with the exponent $\gamma < 1$. Specifically, the value $\gamma = 0.35$ was predicted for conduction with a variable hopping length, and $\gamma = 0.5$ for conduction with a constant activation energy [21,22]. On the other hand, an intriguing Hall insulator state was predicted [1] for 2D electron gas, in which resistance increases to infinity upon lowering the temperature, while the Hall coefficient remains finite and close to the classical value $\rho_{OHE} = 1/n_s e$, where n_s is an areal density of electrons. Our data for $\rho < 10^{-1}\,\Omega$ cm seem to meet the definition of the Hall insulator state with diverging resistance and approximately constant Hall coefficient, although resistivity increases due to oxidation and not by decreasing temperature. A different interpretation of the Hall coefficient independent of resistivity was proposed by Kharitonov and Efetov [24,25] for heterogeneous granular materials with intergranular resistance smaller than the quantum resistance R_Q. The model assumes that Hall voltage is generated within grains only, and in absence of quantum effects, is given by the classical formula $\rho_{OHE} = 1/n^* e$, where n^* differs from the carrier density n inside the grains by a numerical coefficient determined by the shape of the grains and type of granular lattice. Resistivity, on the other hand, is determined by intergranular tunneling. Therefore, scaling between resistivity and Hall resistivity is absent. The predicted absence of scaling in this regime has been observed in granular $NiSiO_2$ mixtures [26]. To the best of our knowledge, the existing models of the hopping Hall effect in macroscopically homogeneous media predict no crossover phenomenon when resistance exceeds any critical value. Also, there is no Hall effect model for the heterogeneous granular material with intergranular resistance larger than R_Q.

We shift now to the extraordinary Hall effect. Recent models of EHE in multiband ferromagnetic metals with diluted impurities [7–9] predict three distinct scaling regimes as a function of conductivity. In the clean regime [$\sigma > 10^6\,(\Omega\text{ cm})^{-1}$], the skew scattering mechanism ($\rho_{EHE} \propto \rho$, or $\sigma_{EHE} \propto \sigma$) is predicted to dominate. The extrinsic side jump and an intrinsic Berry phase mechanisms, both characterized by the ratio $\rho_{EHE} \propto \rho^2$ (or $\sigma_{EHE} = \text{const}$), are expected to be dominant in the intermediate disorder regime [$\sigma \sim 10^4 - 10^6\,(\Omega\text{ cm})^{-1}$]. In the high disorder range [$\sigma < 10^4\,(\Omega\text{ cm})^{-1}$], the intrinsic contribution is strongly decayed, resulting in a scaling relation $\sigma_{EHE} \propto \sigma^{\gamma}$ with $\gamma \sim 1.6$. The theory is based on the use of Bloch wave functions assuming a metallic conduction; hence its results are valid only for ferromagnetic metals in principle. EHE in insulating materials with phonon-assisted hopping conductance was treated in Ref. [10]. Here, EHE was calculated by considering hopping through triads of sites [17] along percolating clusters. Scaling $\sigma_{EHE} \propto \sigma^{\gamma}$ with $1.33 \leqslant \gamma \leqslant 1.76$ has been predicted for arbitrary thermally activated hopping processes including variable range hopping, short-range activation hopping, or tunneling influenced by interactions in the Efros-Shklovskii regime. Thus, universal scaling in the form $\sigma_{EHE} \propto \sigma^{\gamma}$ with $\gamma \sim 1.6$ is anticipated for low conductivity materials regardless of whether their conductivity is metallic or thermally activated. Experimental data accumulated so far for different ferromagnets, including perovskite oxides, spinels, and magnetic semiconductors [8] seem to be in reasonable agreement with these theoretical predictions. Figure 4 presents the absolute value of the extraordinary Hall conductivity in oxidized CoFeB films as a function of longitudinal conductivity. One can clearly distinguish two ranges: (1) $\sigma > 10\,(\Omega\text{ cm})^{-1}$, where $\sigma_{EHE} \propto \sigma^2$, and (2) $\sigma < 10\,(\Omega\text{ cm})^{-1}$, where $\sigma_{EHE} \approx \text{const}$. The seeming permanence of ρ_{EHE} ($\sigma_{EHE} \propto \sigma^2$) is an artifact of the EHE conductivity presentation in logarithmic scale. ρ_{EHE} magnitude increases slightly (factor of 1.8) in mildly oxidized samples when resistivity increases by two orders of magnitude between $6 \times 10^{-4}\,\Omega$ cm and $6 \times 10^{-2}\,\Omega$ cm. With a further increase of resistivity ρ_{EHE} starts dropping, reverses polarity to positive, and grows beyond 1 Ω cm when resistivity reaches $10^2\,\Omega$ cm. The onset of the polarity reversal was found in the sample with sheet resistance $1.2 \times 10^4\,\Omega$, which is remarkably close to the quantum resistance value $R_Q = h/2e^2 \approx 12.9$ kΩ. Thus, in the "high" conductivity range the EHE conductance follows $\sigma_{EHE} \propto \sigma^2$, which is not too far from the expected $\sigma_{EHE} \propto \sigma^{1.6}$. However, the "low" conductivity range, where EHE conductance reverses its polarity and is independent of conductivity, is in striking conflict with any known to us model of EHE. The transition between the two ranges occurs when the resistance exceeds the quantum resistance threshold.

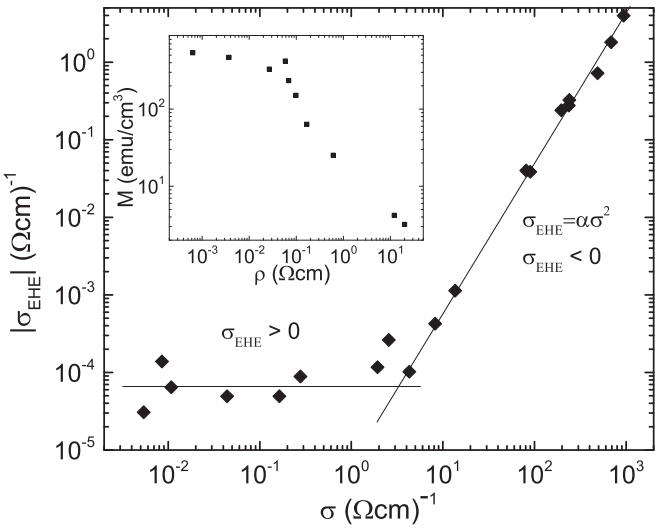

FIG. 4. The absolute value of the EHE conductivity as a function of longitudinal conductivity. Straight lines are a guide to the eye. Inset: magnetization of 50-nm-thick samples as a function of resistivity.

Magnetization of a series of 50-nm-thick samples as a function of their resistivity is shown in the inset of Fig. 4. Magnetization decreases with oxidation from about 600 emu/cm^3 in the nonoxidized sample and drops sharply when the resistivity exceeds the same critical threshold. This

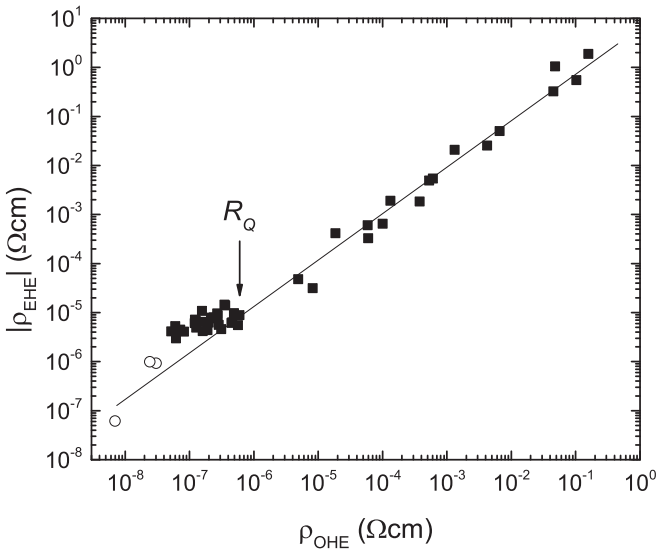

FIG. 5. The absolute value of the EHE resistivity as a function of the ordinary Hall coefficient for multiple series of different thickness. Open symbols correspond to the annealed polycrystalline samples. The slope of the straight line is 1. R_Q marks the crossover threshold.

indicates a clear correlation between the magnetization and the effective density of charge carriers.

Polarity of the Hall effects in the hopping conductance regime was considered in Ref. [27] for hopping of holes between localized states in the impurity band of GaAsMn. In this case, σ_{EHE} was shown to be proportional to the derivative of the density of states at the Fermi energy and therefore expected to change sign as the Fermi level crosses the density-of-states maximum in the impurity band. The ordinary Hall coefficient was predicted to have the same sign everywhere in the impurity band. We find no evidence for a correlation between the density-of-states maximum and crossing the quantum resistance value, therefore the relevance of this model to our case is in question.

It is illuminating to compare the ordinary and the extraordinary Hall effects. Figure 5 presents the absolute magnitude of EHE resistivity as a function of the ordinary Hall coefficient. The figure includes few polycrystalline nonoxidized and slightly oxidized samples fabricated using post-deposition annealing that exhibit Hall effects significantly smaller than amorphous samples. ρ_{EHE} is a linear function of ρ_{OHE} over almost eight orders of magnitude starting from the metallic samples and up to the strongly insulating ones. R_Q marks the crossover threshold, where ρ_{EHE} reverses its polarity and both ρ_{EHE} and ρ_{OHE} start increasing as ρ^2. The linear correlation between ρ_{EHE} and ρ_{OHE} is preserved in the entire range both below and above the threshold. Similar linear correlation between ρ_{EHE} and ρ_{OHE} has been reported in granular $NiSiO_2$ in the metallic and strongly coupled granular ranges [26]. Interpretation of such correlation within the classical single band conduction model would mean that the EHE conductivity is proportional to the charge carrier density, as predicted by Noziéres and Lewiner [28]. However, no such correlation was predicted or even discussed for the hopping or temperature activated tunneling conductance.

The magnitude of the effects is remarkable by itself. Classical models predict the Hall coefficient in metals to depend on the density of carriers and not on the mean free path, and therefore predict no significant changes with resistivity. In granular percolating systems, as the metal concentration approaches the percolation threshold, the Hall coefficient is expected to scale together with conductivity and increase by about tenfold compared with a pure bulk metal. It was surprising when three to four orders enhancement of the extraordinary and the ordinary Hall coefficients have been observed in ferromagnetic granular mixtures $NiSiO_2$ [29] and $FeSiO_2$ [30] and nonmagnetic granular Cu-SiO_2 [6] and Mo-SnO_2 [31]. A local quantum interference theory was suggested [6,32], in which the presence of small insulating substructures along an infinite metallic cluster leads to profound wave scattering and interference, thus causing a significant reduction of the effective carrier density. The model is only valid at low temperatures when quantum corrections (weak localization/electron-electron interaction) are valid, and cannot explain the "giant Hall effect" at room temperature. Here, we find a huge enhancement by almost eight orders of magnitude in both Hall effects, surpassing by large the giant Hall effect in granular systems.

IV. SUMMARY

We can summarize our main findings as follows: (1) Amorphous ferromagnetic CoFeB films can be controllably modified by gradual oxidation between the metallic and the insulating states over six orders of resistivity. Both the ordinary and the extraordinary Hall effects are large enough to be measurable in the strongly insulating state. (2) There exists a critical resistance threshold beyond which three effects have been identified: polarity of the EHE reverses, and both the ordinary Hall coefficient and the extraordinary Hall resistivity amplitudes diverge with resistivity as ρ^2. (3) The critical threshold can be identified as the quantum resistance $h/2e^2$. (4) The EHE resistivity scales linearly with the ordinary Hall coefficient over eight orders of magnitude from the metallic into the strongly insulating state. (5) Both the EHE resistivity and the ordinary Hall coefficient in the oxidized state are huge, exceeding their values in the crystalline metallic state by almost eight orders of magnitude. The scope of the behavior is dramatically different both qualitatively and quantitatively from that experimentally known in other studied materials and from the theoretically predicted. Unfortunately, we were unable to establish the microscopic structure of this amorphous material. Whether it is homogeneous or heterogeneous, i.e., composed of amorphous ferromagnetic clusters embedded within amorphous insulating matrix, is currently not known. One wonders whether the phenomena are a general property of amorphous partially oxidized normal and ferromagnetic metals, and whether this type of materials with a huge magnetic field response and nontrivial effective mobility can be used for practical applications.

ACKNOWLEDGMENTS

We acknowledge the financial support by the XIN center of Tel Aviv and Tsinghua Universities.

[1] S.-C. Zhang, S. Kivelson, and D.-H. Lee, Phys. Rev. Lett. **69**, 1252 (1992).
[2] O. Entin-Wohlman, A. G. Aronov, Y. Levinson, and Y. Imry, Phys. Rev. Lett. **75**, 4094 (1995).
[3] P. Dai, Y. Zhang, and M. P. Sarachik, Phys. Rev. Lett. **70**, 1968 (1993).
[4] P. G. Le Comber, D. I. Jones, and W. E. Spear, Philos. Mag. A **35**, 1173 (1977).
[5] C. Sellmer, T. Bronger, W. Beyer, and R. Carius, J. Non-Cryst. Solids **358**, 2044 (2012).
[6] X. X. Zhang, C. Wan, H. Liu, Z. Q. Li, P. Sheng, and J. J. Lin, Phys. Rev. Lett. **86**, 5562 (2001).
[7] S. Onoda, N. Sugimoto, and N. Nagaosa, Phys. Rev. Lett. **97**, 126602 (2006).
[8] S. Onoda, N. Sugimoto, and N. Nagaosa, Phys. Rev. B **77**, 165103 (2008), and references therein.
[9] N. Nagaosa, J. Sinova, S. Onoda, A. H. MacDonald, and N. P. Ong, Rev. Mod. Phys. **82**, 1539 (2010), and references therein.
[10] X-J. Liu, X. Liu, and J. Sinova, Phys. Rev. B **84**, 165304 (2011).
[11] A. B. Pakhomov, X. Yan, and B. Zhao, Appl. Phys. Lett. **67**, 3497 (1995).
[12] G. Kopnov and A. Gerber, Appl. Phys. Lett. **109**, 022404 (2016).
[13] A. Simons, A. Gerber, I. Ya. Korenblit, A. Suslov, B. Raquet, M. Passacantando, L. Ottaviano, G. Impellizzeri, and A. Aronzon, J. Appl. Phys. **115**, 093703 (2014).
[14] N. F. Mott, *Metal Insulator Transitions* (Taylor & Francis, London, 1974).
[15] I. S. Beloborodov, A. V. Lopatin, and V. M. Vinokur, Phys. Rev. B **72**, 125121 (2005).
[16] N. F. Mott and E. A. Davis, *Electronic Processes in Non-Crystalline Materials*, 2nd ed. (Oxford University Press, New York, 1979), p. 56.
[17] T. Holstein, Phys. Rev. **124**, 1329 (1961).
[18] L. Friedman and M. Pollak, Philos. Mag. B **38**, 173 (1978).
[19] P. Butcher, Philos. Mag. B **42**, 799 (1980).
[20] M. Gruenewald, H. Mueller, P. Thomas, and D. Wuertz, Solid State Commun. **38**, 1011 (1981).
[21] Y. Gal'perin, E. German, and V. Karpov, Sov. Phys. JETP **72**, 193 (1991).
[22] R Németh and B. Mühlschlegel, Solid State Commun. **66**, 999 (1988).
[23] A. Avdonin, P. Skupiński, and K. Grasza, Physica B **483**, 13 (2016).
[24] M. Yu. Kharitonov and K. B. Efetov, Phys. Rev. Lett. **99**, 056803 (2007).
[25] M. Yu. Kharitonov and K. B. Efetov, Phys. Rev. B **77**, 045116 (2008).
[26] D. Bartov, A. Segal, M. Karpovski, and A. Gerber, Phys. Rev. B **90**, 144423 (2014).
[27] A. A. Burkov and L. Balents, Phys. Rev. Lett. **91**, 057202 (2003).
[28] P. Nozières and C. Lewiner, J. Phys. (France) **34**, 901 (1973).
[29] A. B. Pakhomov and X. Yan, Solid State Commun. **99**, 139 (1996).
[30] B. Zhao and X. Yan, J. Appl. Phys. **81**, 4290 (1997).
[31] Y.-N. Wu, Z.-Q. Li, and J.-J. Lin, Phys. Rev. B **82**, 092202 (2010).
[32] C. Wan and P. Sheng, Phys. Rev. B **66**, 075309 (2002).